energies

MDPI

Article

Suction Removal of Cohesionless Sediment

Pu Yang [1], Guorong Wang [1,2,*] and Lin Zhong [1]

[1] Department of Mechatronic Engineering, Southwest Petroleum University, Chengdu 610500, China; stu_yp@163.com (P.Y.); zhonglin858296@163.com (L.Z.)
[2] State Key Laboratory of Oil and Gas Reservoir Geology and Exploitation, Southwest Petroleum University, Chengdu 610500, China
* Correspondence: 200331010023@swpu.edu.cn; Tel.: +86-28-83037227

Received: 8 September 2020; Accepted: 13 October 2020; Published: 18 October 2020

Abstract: The theoretical analysis of sediment scour in vertical direction caused by a vertical suction inlet is presented here. The predictive formulas of the critical inlet height of particle initial motion and scour depth in equilibrium state are expressed as Froude type relations based on the phenomenological theory of turbulence and the momentum transfer hypothesis between fluid and grain. The experimental data of the literature shows good consistency with the theoretical relationship, and the physical mechanism is clear. In addition, the discussion for the applicability of the predictive formula in an extensive range of Reynolds numbers reveals that the sediment incipient motion can be excellently explained by the energy spectrum of the phenomenological theory. Then the theoretical errors in different flow regions are investigated. The research presents universal relevance and reference value for similar research and application.

Keywords: hydraulic suction; cohesionless sediment scour; scour depth

1. Introduction

Hydraulic suction is often used for sediment removal in the field of hydraulic engineering, especially for cohesionless material transport. Examples are traditional suction dredging, deep sea mining operations and hydrosuction dredging. In addition, it has been applied in an attempt to mine non-diagenetic marine gas hydrate as a novel and safe method (the solid fluidization method) [1]. However the studies on theory of the structural design and result forecast lag behind the development of its applications in the projects. Vertical straight tube with cylindrical inlet is the most common and basic operating mode of theoretical research. In this paper, for the basic case, the theoretical work of sediment scour in vertical direction by suction inlet (e.g., the relationship between multiple variables of suction flow and scour depth in critical states) is supplemented.

In order to obtain the predictive formulae of the scour hole under the suction entrance, several empirical studies (e.g., dimensional analysis and data regression based on the experimental results) have been carried out [2–6]. In aspect of theoretical research, the study of Salzman et al. [7] shows that the flow towards the pipe not only across the sand surface but also through the sand bed, and the suction flow is a potential current. Rehbinder [8] and Ullah et al. [9] treated the flow into the tube as a sink by ignoring the effect of the bed deformation on the flow. The physical mechanism of erosion process was studied theoretically based on potential flow and boundary layer theory. Meanwhile the force acting on grain and balance model was obtained. They all calculated the shear stress generated in boundary layer on the surface of the sand bed and considered the force caused by seepage in sediment. Rehbinder [8] focused on understanding the initial motion of sediment particles (the inlet position above the bed). Ullah et al. [9] additionally investigated the influence of the angle of repose of the sediment on the equilibrium state of scour, and focused on assessing the radial erosion

(the relationship between multiple variables of suction flow and radial extent of scour in equilibrium state).

The present theoretical work for the first time investigates the erosion in vertical direction (operating distance of suction entrance) by establishing a shear stress balance model at the bottom of scour hole, according to the phenomenological theory of turbulence and the momentum transfer hypothesis between fluid and grain [10]. There is always a crucial and idealized assumption that the Reynolds number at the bottom of the scour hole is so large that the flow is completely in hydraulic rough region [11,12], which limits the applicability of phenomenological theory. The effect of viscosity is not taken into account in the theoretical model. Thus the experimental data deviating from the theoretical relationship model is valueless in theory when the assumption is failure [12]. The explanation and physical meaning of the deviation are also explored in the present study based on the energy spectrum of the phenomenology theory.

2. Analysis

Typically, the velocity of fluid near the sand bed increases with the decreases of inlet height z_0 when the suction flux Q and inside diameter of tube d keep constant. There is no particle removal and obvious erosion marks along the interface until z_0 decreases to a threshold (critical height). As the inlet height is further decreased, the sediment starts to move obviously [8]. Only the particles below the suction pipe can be lifted off the bed by the flow, because beyond the projection of the inlet exterior margin the pressure gradient at the soil surface is negligibly small [7]. Particles outside the entrance edge are hydraulically transported to the center, but not all of them can be carried into the inlet by the flow. As a result, a small conical sand pile is observed at the stagnation point. Then, a ring-shaped scour trace form around the pile where the horizontal shear force is the maximum along the scour interface. As time progresses, the depth of the ring increases until it reaches the maximum ε_m. Sediment outside the ring is moved or collapses into the hole due to the gravity or hydraulic force triggered by flow across the surface and seepage in sediment, and the diameter of the scour hole increases progressively before an equilibrium is reached in radial direction. If the tube is inserted below the bed initially ($z_0 < 0$), there will be a significant drop of sediment above the inlet level and radial extent of scour hole around the tube in the first few seconds when the flow rate U is set above the critical value [6], and then a deeper scour hole will be observed eventually as shown in Figure 1. The absolute difference between ε_m and z_0 is defined as the net scour depth ε_{rm} in this paper.

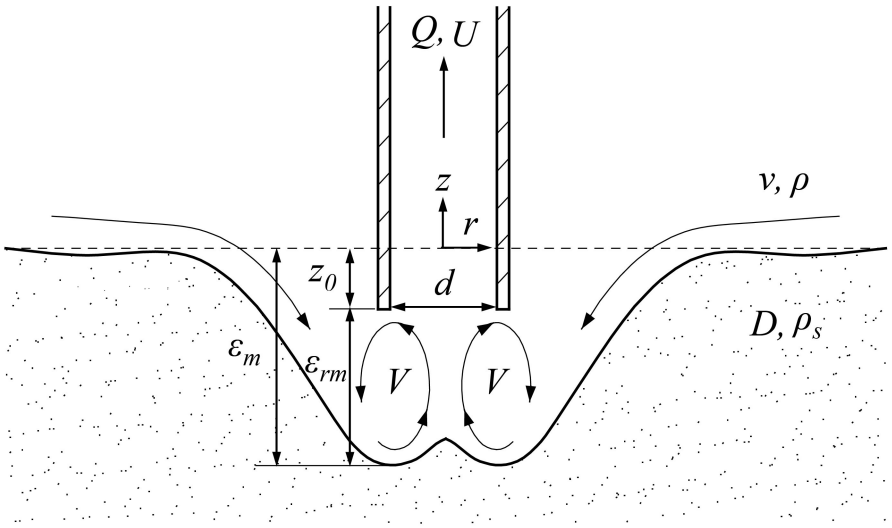

Figure 1. Diagrammatic sketch of erosion by suction flow.

The equilibrium of erosion in vertical direction is the focus of this paper. In the process of vertical erosion, two critical states will be reached with the change of fluid velocity near the interface of fluid and sediment. We first investigate the maximum scour depth of the situation in which the tube inlet is set below the critical height at the beginning. In this case, there will be a balance of hydraulic force and movement resistance on sediment particles at the deepest part of the scour hole where the local slope of the interface is so small that the equilibrium is independent of it [12]. Following the incipient motion theory of Shields [13], equilibrium formula of cohesionless sediment transport can be expressed as

$$(\tau_0)_c = (\rho_s - \rho)gD(\tau_*)_c \tag{1}$$

where τ_0 is the shear stress of flow acting on the interface of fluid and sediment at the deepest part of the scour hole, ρ is the density of water, ρ_s is the density of the sediment particles, D is the diameter of the particles, g is the gravitational acceleration, τ_* is the Shields dimensionless parameter, and subscript letter c represents the critical value. $(\tau_*)_c$ is a function of the Reynolds number $Re^* = VD/\nu$. When the flow is in hydraulic rough region (Re^* exceeds a value), the $(\tau_*)_c$ keeps constant and then $(\tau_0)_c$ scales with $(\rho_s - \rho)gD$. In other words, the movement resistance of grain scales with the gravitational stress $(\rho_s - \rho)gD$, and the hydraulic force is formalized as a shear stress τ_0. A coefficient $(\tau_*)_c$ related to Re^* is measured to correct the effect of viscous layer on critical force $(\tau_0)_c$ in different flow regions.

As shown in Figure 2, The shear stress τ_0 exerted by the flow along the interface can be obtained from the momentum transfer hypothesis. v_n and v_t are respectively defined as the fluctuating velocities which are perpendicular or parallel to the interface. The interface of fluid and sediment is tangent to the peaks of the viscous layer. Bombardelli et al. [14] argue that these velocities are provided by turbulent eddies and τ_0 affected by the momentum transfer of these fluctuating velocities scales with $\rho v_n v_t$. The mathematical form is expressed as

$$\tau_0 \sim \rho v_n v_t \tag{2}$$

We now study these fluctuating velocities of eddies using the phenomenological theory of turbulence, which is applicable to both isotropic and anisotropic turbulence flows [14]. The velocity v_l of the eddies of size l is expressed as $v_l^2 = \int_0^l E(\delta)\delta^{-2}d\delta$, where $E(\delta)$ is the energy spectrum function at a length scale δ and $E(\delta) \sim \varepsilon^{2/3}\delta^{5/3}f_\eta(\eta/\delta)f_L(\delta/L)$ [15]. Here $\varepsilon \sim V^3/L$ is the rate of production or dissipation of turbulent kinetic energy (TKE) per unit mass and it is independent of viscosity within the inertial range ($\eta \ll \delta \ll L$). $\eta = \nu^{3/4}\varepsilon^{-1/4}$ is the viscous length scale, and L is the largest length scale of flow field in depth direction. The size of largest eddies scales with L, and the characteristic velocity of the largest eddies is V. Then we can write $\eta \sim LRe^{-3/4}$, where $Re = VL/\nu$. The TKE of the turbulent cauldron is introduced by the largest eddies and dissipated by eddies smaller than viscous length scale. In other words, TKE cascades from large scales to small scales at same ε in inertial range which widens as Re increases. $f_\eta = e^{-2.1\eta/\delta}$ is a correction function for the dissipative range where $\delta \approx \eta$. $f_L = (1 + 6.783(\delta/L)^2)^{-1/2(5/3+p)}$ is a correction function for the energetic range where $\delta \approx L$ and is known as the Von Karman spectrum with $p = 4$. Obviously, out of the dissipative range ($\eta/\delta \approx 0$), $f_\eta \approx 1$ has no effect on $E(\delta)$, and out of the energetic range ($\delta/L \approx 0$), $f_L \approx 1$ has no effect on $E(\delta)$. This implies that

$$v_l^2 \sim V^2(l/L)^{2/3} \tag{3}$$

which is valid for the inertial range where $E(\delta) \sim \varepsilon^{2/3}\delta^{5/3}$. The well known scaling has been used to reveal the essence of several classical empirical formulas in the field of hydraulics [11].

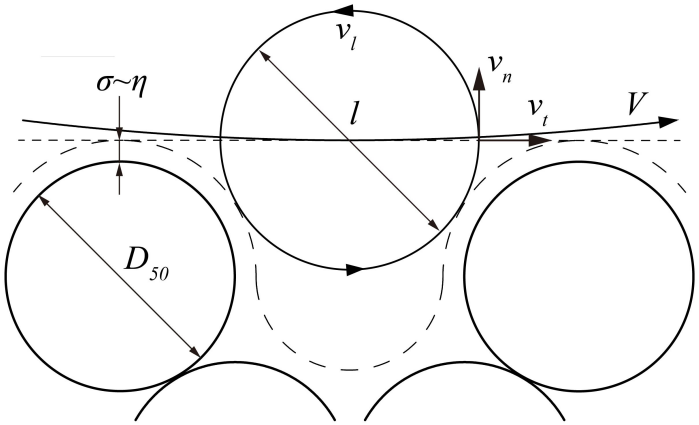

Figure 2. Schematic of eddies triggered by turbulent cauldron on the interface.

Then we go back to these fluctuating velocities lying in the scaling $\tau_0 \sim \rho v_n v_t$. We consider v_t first. Horizontal momentum transfer across the interface can be provided by turbulent eddies of all sizes, Figure 2. The law of energy cascade indicates that the larger the scales of eddies, the greater the momentum of eddies. Thus the horizontal momentum transfer is dominated by V (which is approximately parallel to the interface), and $v_t \sim V$. We now study v_n and define l as the size of largest eddies that occupy the spaces between successive particles and cross the interface vertically. The thickness of viscous layer σ approximately equal to 5η [16]. We assume that Re is so large in scour hole (recall $\eta \sim LRe^{-3/4}$) that $\eta \ll D$ (i.e. the flow is in hydraulic rough region). Then $l \sim D$ can be obtained. When eddies of sizes are much larger than l, the vertical component of momentum transfer across the interface is negligible which can be explained by geometry. Moreover, eddies of sizes much smaller than l is neglected because of the law of energy cascade. Therefore, $v_n \sim v_l \sim v_D \sim V(D/L)^{1/3}$), and hence

$$\tau_0 \sim \rho v_D V \sim \rho V^2 (D/L)^{1/3} \tag{4}$$

The critical state is $\tau_0 = (\tau_0)_c$. By integrating $\tau_0 \sim \rho V^2 (D/L)^{1/3}$ into $(\tau_0)_c \sim (\rho_s - \rho) g D$ and reorganizing, the equilibrium is expressed as

$$V / \sqrt{(\frac{\rho_s - \rho}{\rho}) g D} \sim (\frac{D}{L})^{-1/6} \tag{5}$$

In order to calculate the τ_0 according to the hydraulic parameters operated in engineering or experiments, we assume that L scales with ε_{rm} because the latter is the largest length scale of flow in vertical direction and the target parameter in the present study. The assumption which had been made more than once is a viable option [12]. Next we consider V according to the law of energy conservation. The energy introduced in largest eddies is provided by the suction flow. Therefore the power of suction flow per unit mass (P) equal to the rate of production of TKE ($P/M = \varepsilon \sim V^3/L$). $P = Q\rho g \varepsilon_{rm}$, and the mass of the largest eddies $M \sim \rho L^3$. Thus

$$V \sim (Qg/L)^{1/3} \tag{6}$$

$$V / \sqrt{(\frac{\rho_s - \rho}{\rho}) g D} \sim (\frac{Qg}{\varepsilon_{rm}})^{1/3} / \sqrt{(\frac{\rho_s - \rho}{\rho}) g D} \sim (\frac{D}{\varepsilon_{rm}})^{-1/6} \tag{7}$$

There is a similar critical state in the second situation in which the tube inlet is set above the critical height at the beginning. We now study the initial movement ($z_0 = z_c$) or general movement ($z_0 = z_g$) of particles (two observation criteria for particle initial motion) when the velocity of fluid near the sand bed increases to a threshold value. The two motion states differ only in number of particles transported at the first few seconds. We assume that $\varepsilon_m \approx 0$, and then $\varepsilon_{rm} = \varepsilon_m + z_0 = z_0$. In fact, small traces caused by hydraulic force can be observed on the interface when the particles start to move, but it is difficult to measrue the depth [8]. It is not difficult to understand that the incipient motion analysis in first situation is also suitable for this case. Therefore the dimensionless relationship between critical height and hydraulic parameters is similar to the one derived previously (see the Equation (7)), and expressed as

$$V/\sqrt{(\frac{\rho_s - \rho}{\rho})gD} \sim (\frac{Qg}{z_0})^{1/3}/\sqrt{(\frac{\rho_s - \rho}{\rho})gD} \sim (\frac{D}{z_0})^{-1/6} \tag{8}$$

These relationships can be described as a new Froude type relationship ($Fr = V/\sqrt{(\rho_s - \rho)/\rho gD}$), which doesn't have unknown power exponents. A empirical arguments of Froude relationship have been discovered in experimental data [9]. The mathematical form is expressed as

$$Fr \sim (\frac{D}{L})^{-1/6} \tag{9}$$

where the L scales with ε_{rm}.

Again, it should be noted that these relationships are valid when the fow is in the hydraulic rough region and the length scales of the sediment diameter is within the inertial range. This implies that

$$\eta \ll D \ll L \tag{10}$$

η has been obtained in the previous paragraph.

$$\eta \sim LRe^{-3/4} \tag{11}$$

Therefore Equations (7) and (8) are valid if

$$Re^{-3/4} \ll D/L \ll 1 \tag{12}$$

3. Experimental Results

In order to verify the efficiency of the dimensionless relationship expressed in Equations (7) and (8), the Fr was plotted against the relative roughness ($D/L \sim D/\varepsilon_{rm}$ or D/z_c or D/z_g) according to the experimental data of Ullah [6], as shown in Figures 3 and 4. The sediment particles have the same specific gravity but two sizes. The inlet heights vary from -101.6 mm to 6.4 mm for testing the first critical states. z_c and z_g vary from 3.7 mm to 17.8 mm.

The best fit lines were calculated respectively, and the lines for different particles were almost parallel to each other in each case.The plots indicate that there is a clear power law relation between Fr and relative roughness (D/L) at critical states, which is consistent with the theoretical results. However, the fitted exponents of experimental results are slightly smaller than the theoretical prediction (-0.167).

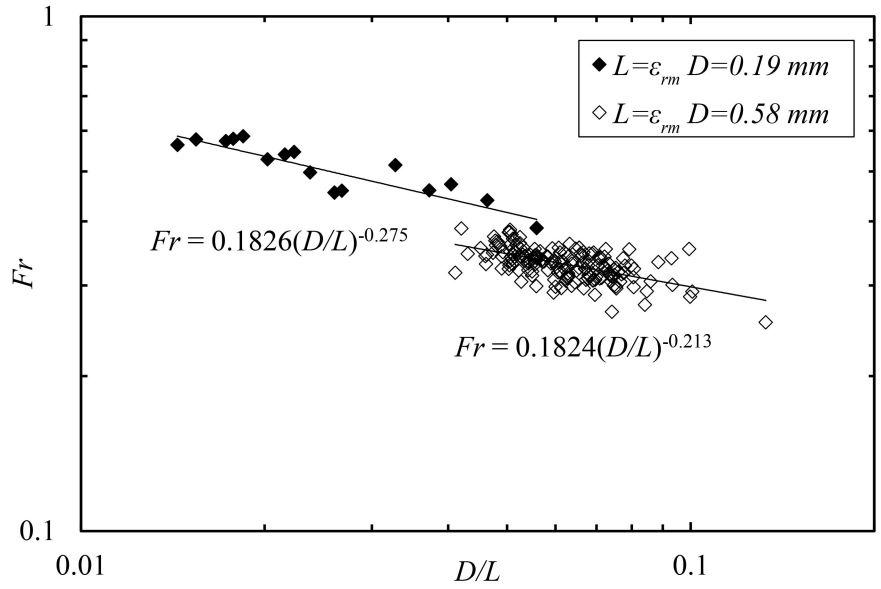

Figure 3. The dimensionless predictive formula of scour depth.

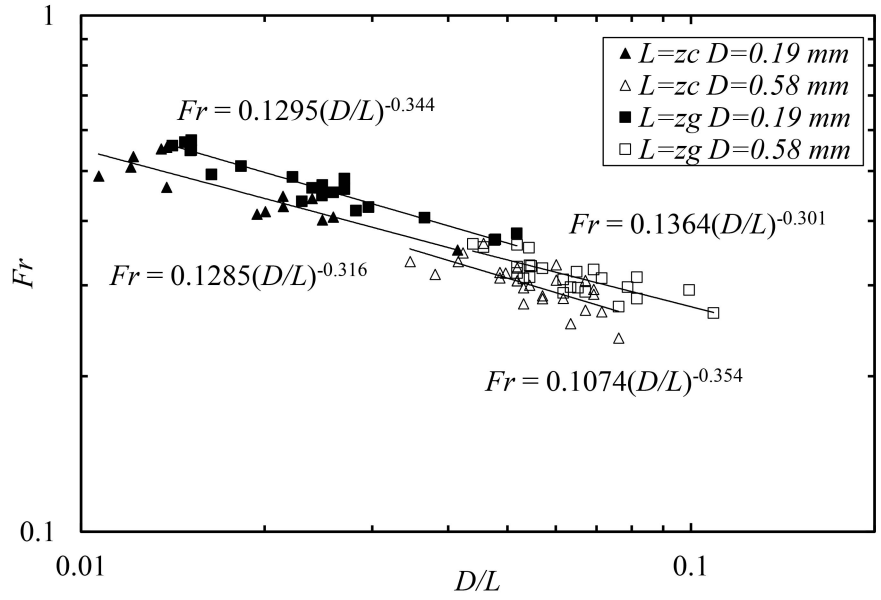

Figure 4. The dimensionless predictive formula of critical inlet height of particle initial motion.

There is an implicit assumption in data processing. Sand bed is considered to be composed of spherical particles, and the diameter of particle D is replaced by the mean grain size D_{50}. In fact, the particles have inconsistency size unevenly distributed. The different exponent values shown in Figures 3 and 4 may be caused by the inevitable error. The research of turbulence laws in natural bed flows [17] report that the 5/3 scaling law ($E(\delta) \sim \delta^{5/3}$) based on highly idealized assumptions may need a slight correction due to the bed roughness heterogeneity and to fluctuation anisotropy. In Equations (7) and (8), the exponent value of the relative roughness is determined to a large degree by the 5/3 scaling law. Therefore, the exponent errors are possibly introduced by the 5/3 scaling law and can be modified by experiment data easily. The power law relation between Fr and relative roughness D/L is still valid.

There is a different phenomenon that the exponent errors in second critical states (as shown in Figure 4) are clearly larger than that in first critical states (as shown in Figure 3). The contrast can not just be explained by the 5/3 scaling law, which indicates that there is a second error. The biggest

difference between the two critical states is the shape of the scour hole which mainly effects the velocity field. The Shields diagram of sediments incipient motion indicates that the simplified assumption (the Reynolds number in critical states is so large that the flow is always in hydraulic rough region) is not always valid. Thus the second error is probably introduced by the turbulence of different development degree, which is discussed in next section.

4. Discussion

Before commenting on the second error we should further estimate the shear stress of flow acting on sediment particles in an extensive range of Reynolds number. The sediment incipient motion analysis based on the phenomenology theory of turbulence will be reconstructed. The assumption of large Reynolds number no longer exists. Thus $E(\delta) \sim \varepsilon^{2/3}\delta^{5/3}e^{-2.1\eta/\delta}(1+6.783(\delta/L)^{-17/6})$. We set $\eta = k_1 LRe^{-3/4}$, where k_1 is dimensionless constant and is assumed equal to 1 due to the lack of experimental data in suction flow field. The revaluated size of eddies l approximately equals to the sum of the diameter of particle and the thickness of viscous layer ($l \approx D + \sigma$) as shown in Figure 2 (recall $\sigma \approx 5\eta$, $\eta \sim LRe^{-3/4}$). Then the v_l can be expressed as

$$v_l \sim V\left(\int_0^{D/L+5Re^{-3/4}} t^{-1/3}e^{-2.1Re^{-3/4}/t}(1+6.783t^2)^{-17/6}\right)^{1/2} \sim V\Psi(Re,t) \tag{13}$$

where $t = \delta/L$. Now we combine $\tau_0 \sim \rho v_l V$ with $(\tau_0)_c = (\rho_s - \rho)gD(\tau_*)_c$. Then the new relationship in critical states for general Reynolds number is expressed as $k_2\rho V^2\Psi(Re,t) = (\rho_s - \rho)gD(\tau_*)_c$. The function value of $\Psi(Re,t)$ is plotted against the Re, and some typical curves are shown in Figure 5.

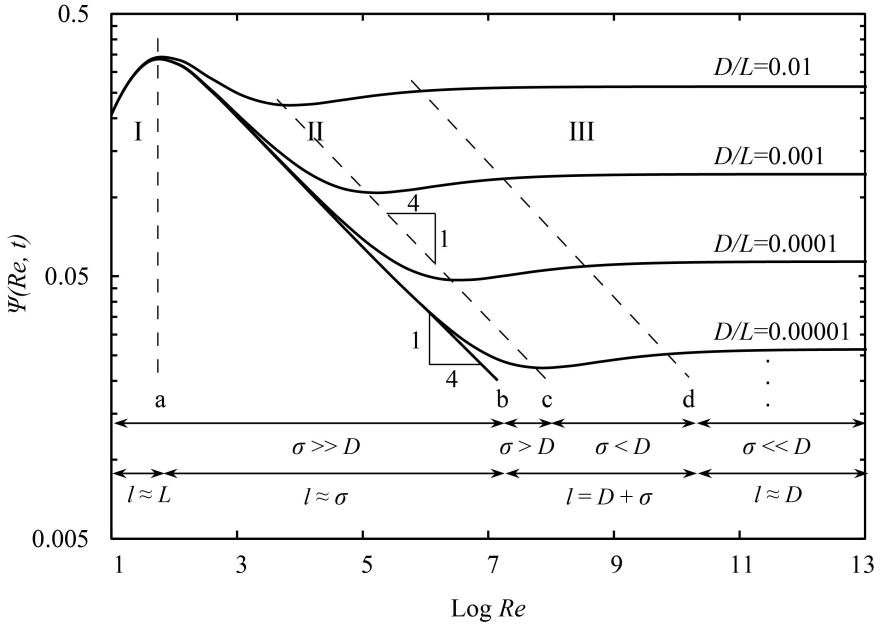

Figure 5. The function value, $\Psi(Re,t)$, plotted against Re for four typical relative roughness: $D/L = 0.01$; $D/L = 0.001$; $D/L = 0.0001$; $D/L = 0.00001$.

The function curves in zone II and III (right side of line a) show an excellent qualitative agreement with Shields diagram. The change of k_1 and k_2 in a wide range does not qualitatively affect the trend of these curves, which means that $\Psi(Re,t)$ can be regarded as the same as the Shields number to correct the effect of viscous layer on τ_0 in different flow region. Thus the sediment incipient motion can be studied with a mathematical analysis using the function $\Psi(Re,t)$. When the spectrum function $E(\delta)$ has no correction for energetic range ($\delta \approx L$), these curves have no variations except zone I which does not exist in Shields diagram. The curves in zone I indicate that the shear stress τ_0 is irrelevant to

relative roughness when the flow is approximately laminar. Zone II (the region between line a and d) is a transition region where the curves are mainly affected by the correction function of dissipative range ($\delta \approx \eta$). The $-1/4$ scaling law (line b) in zone II has a great agreement with Blassius's empirical scaling of hydraulic smooth region [16]. With the increase of Reynolds number, thickness of viscous layer decreases gradually (recall $\eta \sim LRe^{-3/4}$, $\sigma \approx 5\eta$). When the thickness of viscous layer equals to the particle diameter ($\sigma = D_{50}$), the sheer stress attains the minimum. The line (denoted as c) through all these minimum points is parallel to line b. As the Reynolds number continues to increase (recall $l \approx D + \sigma$), the turbulence eddies gradually enter into the clearance of each pair consecutive particles and the turbulence moment transfer increases until the flow is completely in hydraulic rough region (zone III).

Now the flow condition related error can be explained by the energy spectrum of the phenomenological theory. The scour depth varies widely with the change of hydraulic parameters operated in experiments, but the Reynolds number around particles should be approximately always the same in the same critical states when the physical parameters of sediment remains unchanged. Based on $v_l \sim V\Psi(Re, t)$, the Equations (7) and (8) are reorganized and expressed as $V/\sqrt{(\rho_s - \rho)/\rho g D} \sim \Psi^{-1/2}(Re, t)$. The function value of $\Psi^{-1/2}(Re, t,)$ is plotted against the relative roughness (D/L) and some typical curves are shown in Figure 6, which demonstrates the relationship between relative roughness and Fr in an extensive range of Reynolds number. The line c in Figure 5 is plotted again (denoted by c* in Figure 6). Line c* is tangent to all curves, the slope of which is $-1/6$. Figure 6 shows that these curves do not always keep power-law relation with D/L as predicted by Equations (7) and (8) except the right part of each tangent point where the curve is approximately straight (the exponent of D/L approximately eaual to $-1/6$). The larger the Reynolds number, the smaller the value of relative roughness of the tangent point. In fact, comparative analysis of Figures 5 and 6 shows that the $-1/6$ power law is only valid when the data points are completely in zone III (the complete $-5/3$ scaling region as shown in Figure 5 or condition (12)), which is the origin of the second error. When the data points are located at the region between line c and d (shown in Figure 5), the exponent of the relative roughness will be slightly smaller than $-1/6$ (shown in Figure 6). When the data points are located at the region between line b and c, these associated curves shown in Figure 6 are in transient state, and Fr keep a complex relation with relative roughness. When the data points are located at hydraulic smooth region or the left side of line b, these associated curves shown in Figure 6 tend to be straight again, but the exponent of the relative roughness equals to zero. It can be seen that these features are the direct embodiment of the energy distribution of turbulence determined by energy spectrum function of the phenomenology theory.

The Equations (7) and (8) are just valid in a finite interval of relative roughness as shown in the condition (12) which has been explained mathematically by Figures 5 and 6. The boundary values of the condition (12) are strongly correlated in local scour Reynolds number. Because of the missing values of Reynolds number in current literature, the boundary values are not obtained quantitatively. In this paper, we assumed that the data points of Figures 3 and 4 are all located in the right side of line d (shown in Figure 5) which should be the left-sided limits of condition (12). Therefore Figures 3 and 4 show that D/L and Fr dispaly a power law relation, but the associated exponent has error. In fact, for the particles with the same size the Fr in first critical state is larger than that in second critical state. It means that the first critical state has larger lacal scour Reynolds number around particles. This is why the exponents in first critical state are closer to the theoretical value than that in second critical state.

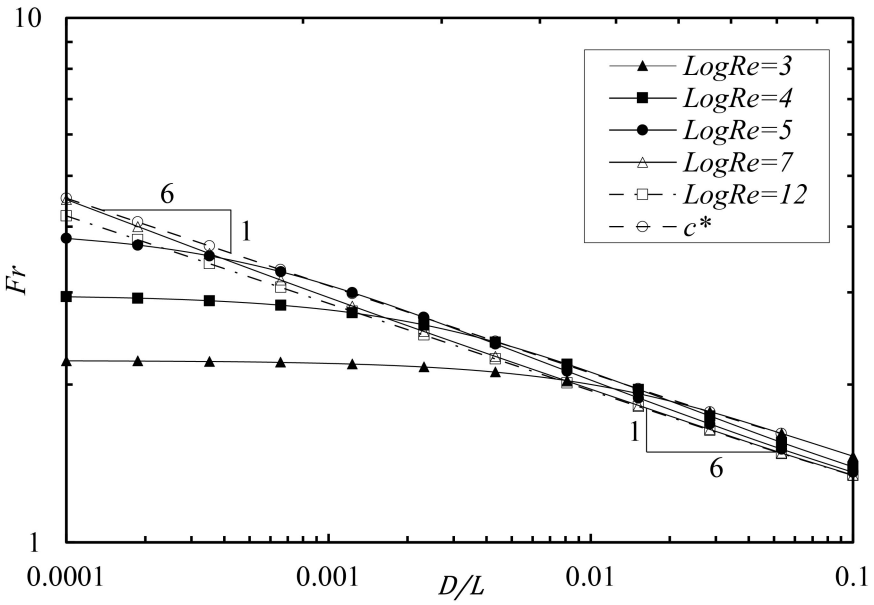

Figure 6. The function value, $\Psi^{-1/2}(Re, t)$, plotted against D/L for several typical Reynolds number.

5. Conclusions

This theoretical work investigates two critical states in the process of cohesionless sediment scour caused by suction flow using the phenomenological theory of turbulence and the momentum transfer hypothesis between fluid and grain. The relationship between critical inlet height, scour depth, sediment physical parameters and operated hydraulic parameters was presented and expressed as a new Froude type scaling. Compared with the empirical approaches (e.g., dimensional analysis and data regression), present new relationship has no issue of scaling between the prototype and the model, in which the power exponents are obtained theoretically and the physical mechanism is clear. The validity and rationality of present analysis based on the phenomenological theory are demonstrated by Shields diagram of sediment incipient motion. In order to explain the slight deviation between experimental data of literature and predictive value in present study, the change of hydraulic force acting on particle in different flow regions gets a satisfactory explanation based on the energy spectrum function of the phenomenological theory. The idealized assumptions of Reynolds number and sediment particles for practical condition are the origins of the theoretical errors. Rather than providing an accurate formula, we pay more attention to the new analysis method, which is helpful for development of general models in an extensive range of Reynolds numbers. While the research is presented based on the simplest structure of the suction inlet, it is the basis of complicated technology and further research.

Author Contributions: Conceptualization, P.Y. and G.W.; methodology, P.Y., G.W. and L.Z.; software, P.Y.; validation, P.Y., G.W. and L.Z.; formal analysis, P.Y.; investigation, P.Y., G.W. and L.Z.; resources, P.Y. and L.Z.; data curation, P.Y.; writing—original draft preparation, P.Y.; writing—review and editing, P.Y., G.W. and L.Z.; visualization, P.Y.; supervision, G.W.; project administration, G.W.; funding acquisition, G.W. All authors have read and agreed to the published version of the manuscript.

Funding: This research was funded by National Key R&D Project (2019YFC0312305) and Zhanjiang Bay laboratory (ZJW-2019-03).

Acknowledgments: We acknowledge the anonymous referees to improve the clarity of the manuscript.

Conflicts of Interest: The authors declare no conflict of interest.

Abbreviations

The following abbreviations are used in this manuscript:

ε_m	maximum scour depth
ε_{rm}	net scour depth
z_0	height of suction entrance above sand bed
z_c	critical inlet height of initial movement
z_g	critical inlet height of general movement
d	inside diameter of tube
Q	suction flux
U	flow rate
D	diameter of the sediment particles
D_{50}	mean grain size of sediment
g	acceleration of gravity
ρ	density of water
ρ_s	density of sediment
ν	kinematic viscosity of fluid
τ_0	shear stress of flow acting on the interface of fluid and sediment at the deepest part of the scour hole
τ_*	Shields dimensionless parameter
V	characteristic velocity of the largest eddies
L	the largest length scale of flow field in depth direction
l	size of one type eddies
v_l	velocity of the eddies of size l
δ	a length scale
$E(\delta)$	energy spectrum function at a length scale δ
ε	rate of production or dissipation of turbulent kinetic energy
η	viscous length scale
σ	thickness of viscous layer
f_η	a correction function for the dissipative range
f_L	a correction function for the energetic range
v_t	fluctuating velocities which are parallel to the interface
v_n	fluctuating velocities which are perpendicular to the interface
Re	Reynolds number

References

1. Wang, G.; Huang, R.; Zhong, L.; Wang, L.; Zhou, S.; Liu, Q. An optimal design of crushing parameters of marine gas hydrate reservoirs in solid fluidization exploitation. *Nat. Gas Ind.* **2019**, *6*, 257–261. [CrossRef]
2. Slotta, L.S. Flow visualization techniques used in dredge cutterhead evaluation. In Proceedings of the 1968 World Dredging Conference (WODCON II), Amsterdam, The Netherlands, 16–18 October 1968; pp. 56–77.
3. Gladigau, L.N. Interactions between sand and water. In Proceedings of the Sixth World Dredging Conference (WODCON VI), Amsterdam, The Netherlands, 7–9 September 2015; pp. 261–294.
4. Brahme, S.B. Environmental Aspects of Suction Cutterheads. Ph.D. Thesis, Texas A&M University, College Station, TX, USA, 1983.
5. Brahme, S.B.; Herbich, J.B. Hydraulic model studies for suction cutterheads. *J. Waterw. Port Coast. Ocean Eng.* **1986**, *112*, 591–606. [CrossRef]
6. Ullah, S.M. Siphon Removal of Cohesionless Materials. MASc Thesis, University of Windsor, Windsor, ON, Canada, 2003.
7. Salzman, H.; Adam, G.M.; Bacdo, D.R. *A Laboratary Study of Fluid and Soil Mechanics Processes during Hydraulic Dredging*; TAMU-SG-77-204, CDS Report No.184; Texas A&M University: College Station, TX, USA, 1977.
8. Rehbinder, G. Sediment removal with a siphon at critical flux. *J. Hydraul. Res.* **1994**, *132*, 854–860. [CrossRef]
9. Ullah, S.M.; Mazurek, K.A.; Rajaratnam, N.; Reitsma, S. Siphon removal of cohesionless materials. *J. Waterw. Port Coast. Ocean Eng.* **2008**, *10*, 142–149. [CrossRef]

10. Gioia, G.; Bombardelli, F.A. Scaling and similarity in rough channel flows. *Phys. Rev. Lett.* **2002**, *88*, 014501. [CrossRef] [PubMed]
11. Ali, S.Z.; Dey, S. Impact of phenomenological theory of turbulence on pragmatic approach to fluvia hydraulics. *Phys. Fluids* **2018**, *30*, 045105. [CrossRef]
12. Manes, C.; Brocchini, M. Local scour around structure and the phenomenology of turbulence. *J. Fluid Mech.* **2015**, *779*, 309–324. [CrossRef]
13. Shields, A.F. *Application of Similarity Principles and Turbulence Research to Bed-Load Movement*; Technical Report; California Institute of Technology: Pasadena, CA, USA, 1936; Volume 26, pp. 5–24.
14. Bombardelli, F.A.; Gioia, G. Scouring of granular beds by jet-driven axisymmetric turbulent cauldrons. *Phys. Fluids* **2006**, *18*, 088101. [CrossRef]
15. Pope, S.B. *Turbulent Flows*, 1st ed.; Cambrige University Press: Cambrige, UK, 2000; pp. 229–237.
16. Gioia, G.; Chakraborty, P. Turbulent friction in rough pipes and the energy spectrum of the phenomenological theory. *Phys. Rev. Lett.* **2006**, *96*, 044502. [CrossRef] [PubMed]
17. Ferraro, D.; Servidio, S.; Carbone, V.; Dey, S.; Gaudio, R. Turbulent friction in rough pipes and the energy spectrum of the phenomenological theory. *Turbul. Laws Nat. Bed Flows* **2016**, *798*, 540–571.